Electronic Supplementary Material (ESI) for Inorganic Chemistry Frontiers.


# Unravelling the role of triisopropylphosphane telluride in Ag(I) complexes

Juan Carlos Pérez-Sánchez,[a,b] Carmen Ceamanos,[a] Raquel P. Herrera,[b] and M. Concepción Gimeno*[a]

[a] *Departamento de Química Inorgánica. Instituto de Síntesis Química y Catálisis Homogénea (ISQCH), CSIC-Universidad de Zaragoza. C/ Pedro Cerbuna 12, E-50009 Zaragoza, Spain.* gimeno@unizar.es

[b] *Laboratorio de Organocatálisis Asimétrica, Departamento de Química Orgánica. Instituto de Síntesis Química y Catálisis Homogénea (ISQCH), CSIC-Universidad de Zaragoza. C/ Pedro Cerbuna 12, E-50009 Zaragoza, Spain.*

## Supporting Information

### Table of Contents

# 1. Experimental Section

**General procedures and materials**: All experiments and manipulations were carried out under argon atmosphere using standard Schlenk techniques. $^{1}H$, $^{19}F$ and $^{31}P$ NMR spectra were recorded on a Bruker Avance 300, 400 or 500 spectrometers at the indicated frequencies at 298.15K, unless otherwise stated. Chemical shifts are reported in ppm and referenced to $SiMe_4$, using the internal signal of the deuterated solvent as reference ($^{1}H$) and external $H_3PO_4$ 85% ($^{31}P$) or external $CFCl_3$ ($^{19}F$). Multiplicity of the observed signals is indicated as follows: s = singlet, br s = broad singlet, d = doublet, dd = doublet of doublets, d sept = doublet of septets, m = multiplet. *J* values are given in Hz. Infrared spectra were recorded (in solid) in the range 4000–250 $cm^{-1}$ on a PerkinElmer Spectrum 100 FTIR spectrometer equipped with an ATR accessory. High resolution mass spectra of complexes were acquired on a Bruker MicroTOF-Q (ESI+) spectrometer. Electrochemical experiments were performed by means of an EG&G Research Model 273 potentiostat/galvanostat. A three-electrode glass cell consisting of a glassy carbon disk working electrode, a platinum-wire auxiliary electrode, and a Ag/AgCl (3 M) reference electrode was employed. The supporting electrolyte solution ($NBu_4PF_6$, 0.1 M) was scanned over the solvent window ($CH_2Cl_2$) to ensure the absence of electroactive impurity curves. A concentration of complex **4** of about $5 \times 10^{-4}$ M was employed in all the measurements. A total of five cycles were acquired for each respective scan rate. All solvents were degassed and dried prior using over activated 3 or 4 Å molecular sieves. Deuterated solvents were purchased from Sigma-Aldrich, dried and stored over molecular sieves (4 Å). All chemical reagents were purchased from commercial suppliers and used as received. The starting materials [Ag(OTf)($PPh_3$)],[1] [Ag(OTf)(μ-dppf)][2] and $TeP(^{i}Pr)_3$[3] were prepared according to published procedures. All other reagents were commercially available and were used without further purification.

**Crystallography.** Crystals suitable for X ray studies were obtained by diffusion of *n*-hexane (**3**) or diethyl ether (**4**) over a solution of the corresponding compound in acetone (**3**) or dichloromethane (**4**), respectively. Crystals were mounted on a MiTeGen Crystal micromount and transferred to the cold gas stream of a Bruker D8 VENTURE diffractometer. Data were collected using monochromated MoKα radiation ($\lambda = 0.71073$ Å). Scan type ω. Absorption correction based on multiple scans were applied with the program SADABS.[4] The structures were refined on $F^2$ using the program OLEX2.[5] All non-hydrogen atoms were refined anisotropically. Hydrogen atoms were included using a riding model. CCDC deposition numbers 2271147 (**3**) and

2271148 (**4**) contain the supplementary crystallographic data. These data can be obtained free of charge by The Cambridge Crystallography Data Center.

**General procedure for the synthesis of complexes 1–2:** To a flame dried Schlenk flask equipped with a stirring bar was added $TeP(^iPr)_3$ (56 mg, 0.2 mmol for **1**; or 112 mg, 0.4 mmol for **2**) and 20 mL of $CH_2Cl_2$. Then [Ag(OTf)($PPh_3$)] (104 mg, 0.2 mmol) was added and the resulting greenish solution was stirred for 30 min protected from light. After this time, the solution was filtered through a 0.45 µm nylon syringe filter and all the volatiles were removed under reduced pressure. The resulting yellow solid was purified through washings with *n*-hexane (2 x 5 mL) and dried under vacuum.

**Complex 1**: Yield (105 mg, 65%). **$^1$H NMR** (300 MHz, $CD_2Cl_2$) $\delta_H$ (ppm): 7.58 – 7.28 (m, 15H, Ph), 2.28 (m, 3H, C***H***$(CH_3)_2$), 1.23 (dd, $^3J_{H,P}$ = 17.5 Hz, $^3J_{H,H}$ = 7.1 Hz, 18H, CH(C***H***$_3)_2$). **$^{31}$P{$^1$H} NMR** (121 MHz, $CD_2Cl_2$, 25 °C) $\delta_P$ (ppm): 48.3 (s, 1P, $P^iPr_3$, $^1J(^{31}P\text{-}^{125}Te)$ = 1384.2 Hz), 9.9 (br s, 1P, $PPh_3$). **$^{19}$F NMR** (282 MHz, $CD_2Cl_2$) $\delta_F$ (ppm): –78.7 (s, 3F, OTf). **HRMS (ESI/QTOF)** m/z: $[M]^+$ Calcd. for $C_{27}H_{36}AgP_2Te$ 659.0400; Found 659.0392. **Elemental analysis** (%) calcd. for $C_{28}H_{36}AgF_3O_3P_2STe$, C: 41.67, H: 4.50, S: 3.97; found C: 41.89, H: 4.91, S: 3.83.

**Complex 2**: Yield (147 mg, 67%). **$^1$H NMR** (300 MHz, $CD_2Cl_2$) $\delta_H$ (ppm): 7.55 – 7.32 (m, 15H, Ph), 2.30 (m, 6H, C***H***$(CH_3)_2$), 1.25 (dd, $^3J_{H,P}$ = 17.1 Hz, $^3J_{H,H}$ = 7.1 Hz, 36H, CH(C***H***$_3)_2$). **$^{31}$P{$^1$H} NMR** (121 MHz, $CD_2Cl_2$, 25 °C) $\delta_P$ (ppm): 43.8 (s, 2P, $P^iPr_3$, $^1J(^{31}P\text{-}^{125}Te)$ = 1481.0 Hz), 6.8 (br s, 1P, $PPh_3$). **$^{19}$F NMR** (282 MHz, $CD_2Cl_2$) $\delta_F$ (ppm): –78.9 (s, 3F, OTf). **Elemental analysis** (%) calcd. for $C_{37}H_{57}AgF_3O_3P_3STe_2$, C: 40.59, H: 5.25, S: 2.93; found C: 40.85, H: 5.61, S: 2.87.

**Synthesis of complex 3:** To a flame dried Schlenk flask equipped with a stirring bar was added $TeP(^iPr)_3$ (112 mg, 0.4 mmol) and 20 mL of $CH_2Cl_2$. Then Ag(OTf) (104 mg, 0.2 mmol) was added, and the resulting greenish solution was stirred for 15 min protected from light. After this time, the solution was filtered through a 0.45 µm nylon syringe filter and it was concentrated under reduced pressure to *ca.* 1 mL. Then *n*-hexane (10 mL) was added to precipitate a yellow solid which was purified through washings with *n*-hexane (2 x 5 mL) and dried under vacuum.

**Complex 3**: Yield (193 mg, 58%). **$^1$H NMR** (300 MHz, $CD_2Cl_2$) $\delta_H$ (ppm): 2.44 (d sept, $^2J_{H,P}$ = 9.6 Hz, $^3J_{H,H}$ = 7.0 Hz, 12H, C***H***$(CH_3)_2$), 1.23 (dd, $^3J_{H,P}$ = 17.5 Hz, $^3J_{H,H}$ = 7.1 Hz, 36H, CH(C***H***$_3)_2$). **$^{31}$P{$^1$H} NMR** (121 MHz, $CD_2Cl_2$, 25 °C) $\delta_P$ (ppm): 47.2 (s, 4P, $P^iPr_3$, $^1J(^{31}P\text{-}^{125}Te)$ = 1386.7 Hz). **$^{19}$F NMR** (282 MHz, $CD_2Cl_2$) $\delta_F$ (ppm): –78.8 (s, 3F, OTf). **HRMS (ESI/QTOF)** m/z: $[M]^{2+}$ Calcd. for $C_{36}H_{84}Ag_2P_4Te_4$ 684.9907; Found $[1/2\ M]^+$ 684.9963 ($C_{18}H_{42}AgP_2Te_2$). **Elemental analysis** (%) calcd. for $C_{38}H_{84}Ag_2F_6O_6P_4S_2Te_4$, C: 27.38, H: 5.20, S: 3.85; found C: 27.30, H: 5.29, S: 3.80,

**General procedure for the synthesis of complexes 4–5:** To a flame dried Schlenk flask equipped with a stirring bar was added $TeP(^{i}Pr)_3$ (56 mg, 0.2 mmol for **4;** or 112 mg, 0.4 mmol for **5**) and 20 mL of $CH_2Cl_2$. Then [Ag(OTf)(μ-dppf)] (162 mg, 0.2 mmol) was added and the resulting orange solution was stirred for 30 min protected from light. After this time, all the volatiles were removed under reduced pressure. The resulting yellow solid was purified through washings with *n*-hexane (2 x 5 mL) and dried under vacuum.

**Complex 4**: Yield (170 mg, 77%). **$^{1}$H NMR** (300 MHz, $CD_2Cl_2$) $\delta_H$ (ppm): 7.55 – 7.41 (m, 20H, dppf – Ph), 4.59 – 4.07 (m, 8H, AA'BB' spin system, dppf – $C_5\boldsymbol{H}_4$-), 2.25 – 2.07 (m, 3H, -C***H***$(CH_3)_2$), 1.18 (dd, $^{3}J_{H,P}$ = 17.3 Hz, $^{3}J_{H,H}$= 7.0 Hz, 18H, -CH(C***H***$_3)_2$). **$^{31}$P{$^{1}$H} NMR** (121 MHz, $CD_2Cl_2$, 25 °C) $\delta_P$ (ppm): 44.9 (s, 1P, $P^{i}Pr_3$, $^{1}J(^{31}P\text{-}^{125}Te)$ = 1450.8 Hz), -0.4 (br s, 2P, dppf). **$^{19}$F NMR** (282 MHz, $CD_2Cl_2$) $\delta_F$ (ppm): –78.9 (s, 3F, OTf). **HRMS (ESI/QTOF)** m/z: $[M]^+$ Calcd. for $C_{43}H_{49}AgFeP_3Te$ 951.0505; Found 951.0526. **Elemental analysis** (%) calcd. for $C_{44}H_{49}AgF_3FeO_3P_3STe$, C: 48.08, H: 4.49, S: 2.92; found C: 47.99, H: 4.72, S: 3.28.

**Complex 5**: Yield (222 mg, 80%). **$^{1}$H NMR** (300 MHz, $CD_2Cl_2$) $\delta_H$ (ppm): 7.54 – 7.38 (m, 20H, dppf – Ph), 4.43 – 4.24 (m, 8H, AA'BB' spin system, dppf – $C_5\boldsymbol{H}_4$-), 2.18 (d sept, $^{2}J_{H,P}$ = 10.3 Hz, $^{3}J_{H,H}$ = 7.3 Hz, 6H, -C***H***$(CH_3)_2$), 1.21 (dd, $^{3}J_{H,P}$ = 16.8 Hz, $^{3}J_{H,H}$ = 7.3 Hz, 36H, -CH(C***H***$_3)_2$). **$^{31}$P{$^{1}$H} NMR** (121 MHz, $CD_2Cl_2$, 25 °C) $\delta_P$ (ppm): 42.6 (s, 2P, $P^{i}Pr_3$, $^{1}J(^{31}P\text{-}^{125}Te)$ = 1182.2 Hz), –2.4 (br s, 2P, dppf). **$^{19}$F NMR** (282 MHz, $CD_2Cl_2$) $\delta_F$ (ppm): –78.9 (s, 3F, OTf). **Elemental analysis** (%) calcd. for $C_{53}H_{70}AgF_3FeO_3P_4STe_2$, C: 45.90, H: 5.09, S: 2.31; found C: 45.96, H: 5.52, S: 2.67.

# 2. NMR and FTIR Spectral Data

**Complex 1**

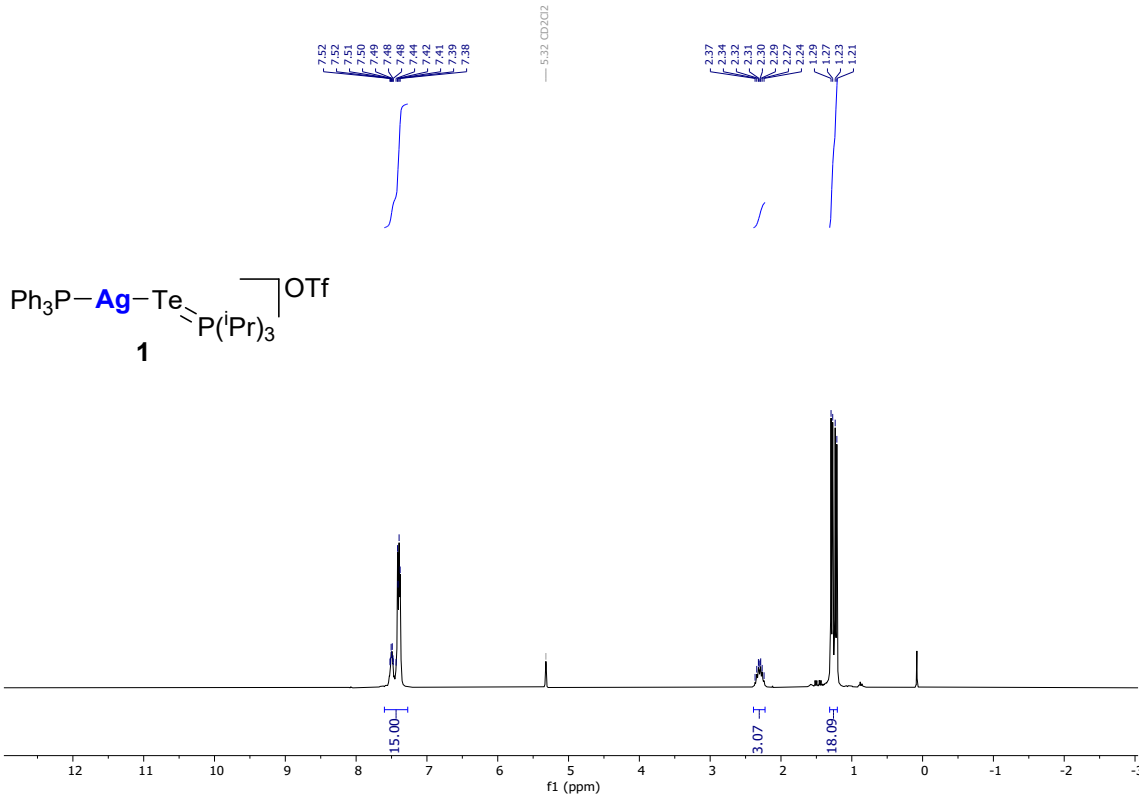


**Figure S1**. $^{1}H$ NMR (300 MHz, $CD_2Cl_2$, 25 °C) spectrum of complex **1**.

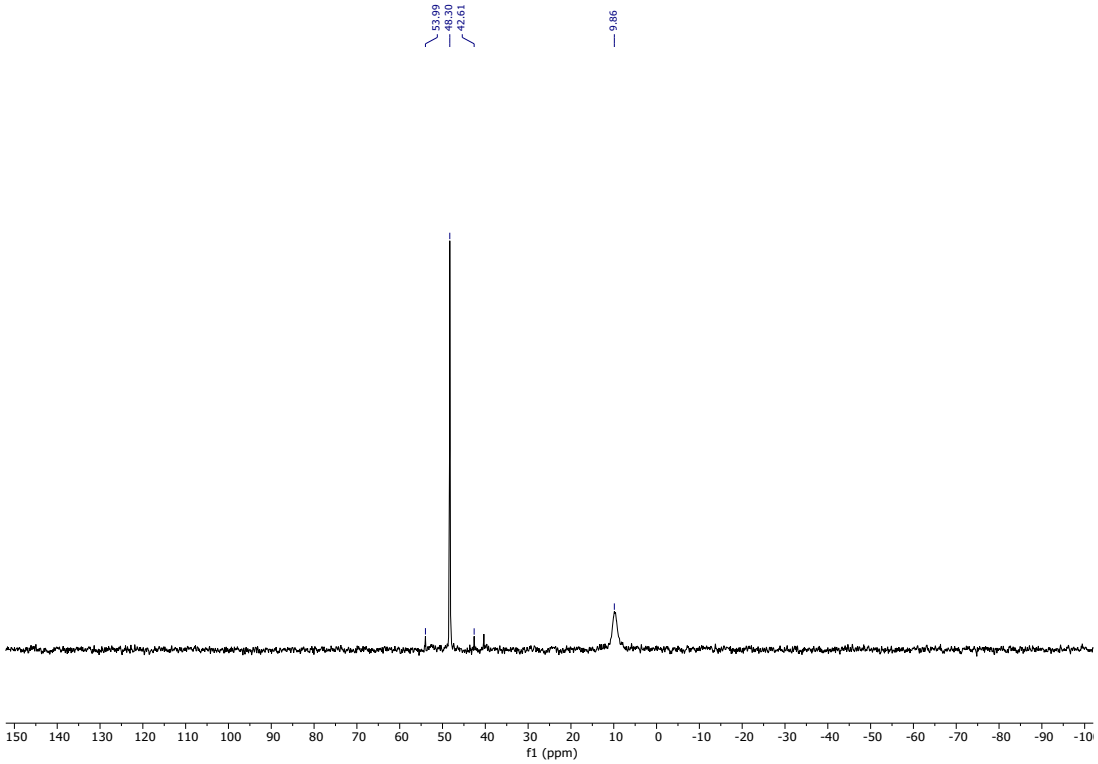


**Figure S2**. $^{31}P\{^{1}H\}$ NMR (121 MHz, $CD_2Cl_2$, 25 °C) spectrum of complex **1**.

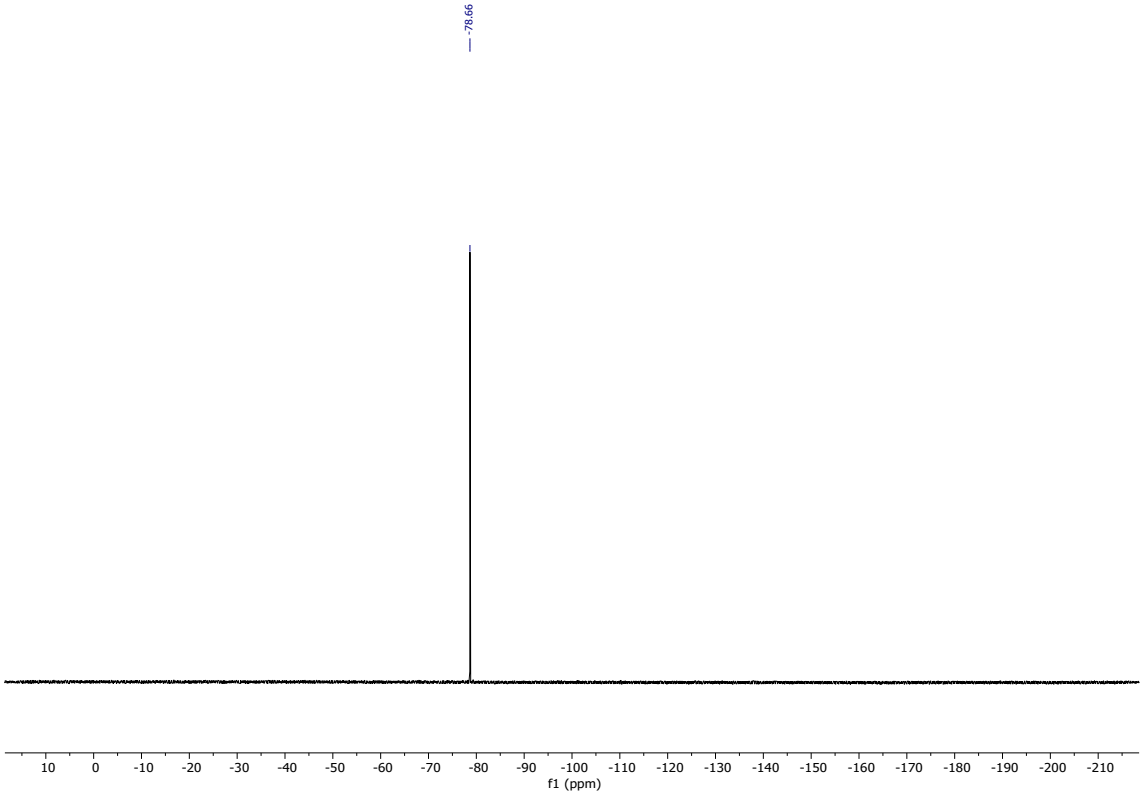


**Figure S3**. $^{19}F$ NMR (282 MHz, $CD_2Cl_2$, 25 °C) spectrum of complex **1**.

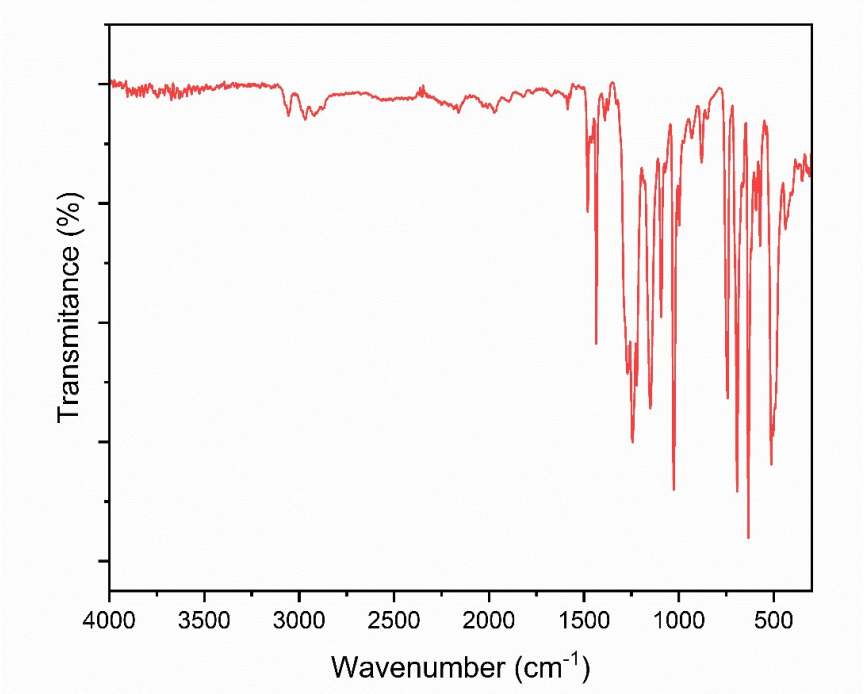


**Figure S4**. FTIR (ATR) spectrum of complex **1**.

**Complex 2**

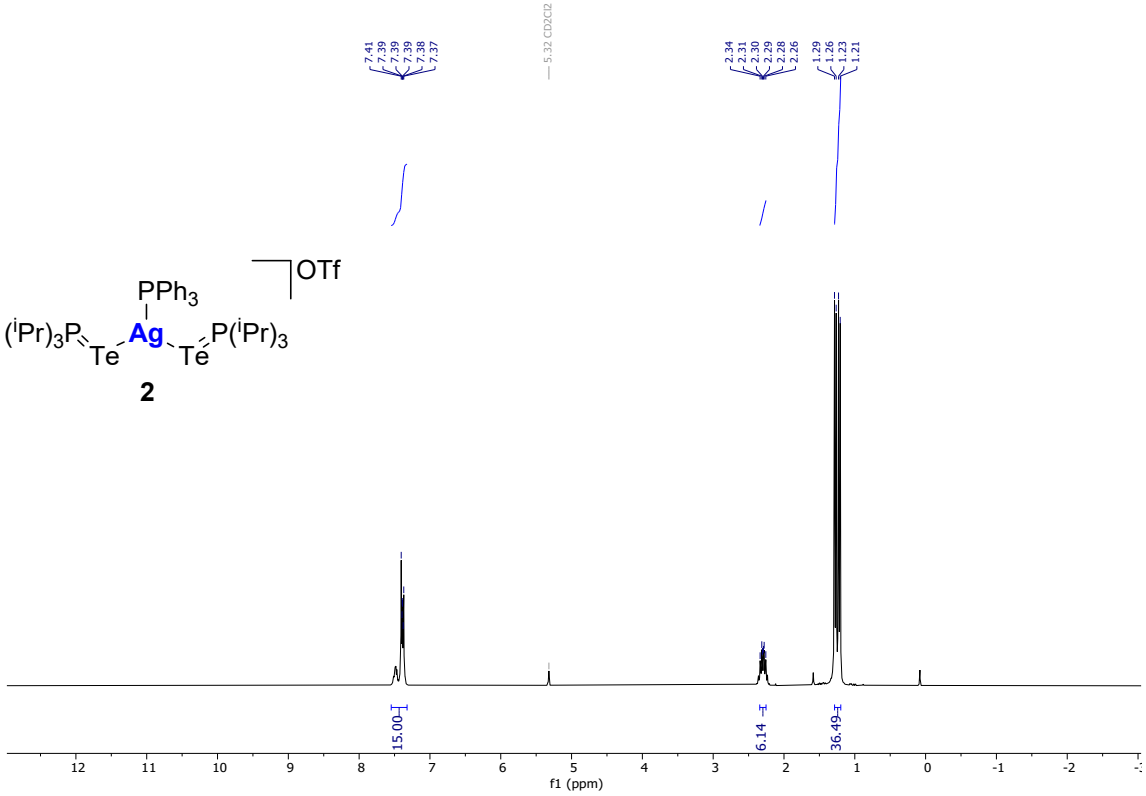


**Figure S5**. $^{1}H$ NMR (300 MHz, $CD_2Cl_2$, 25 °C) spectrum of complex **2**.

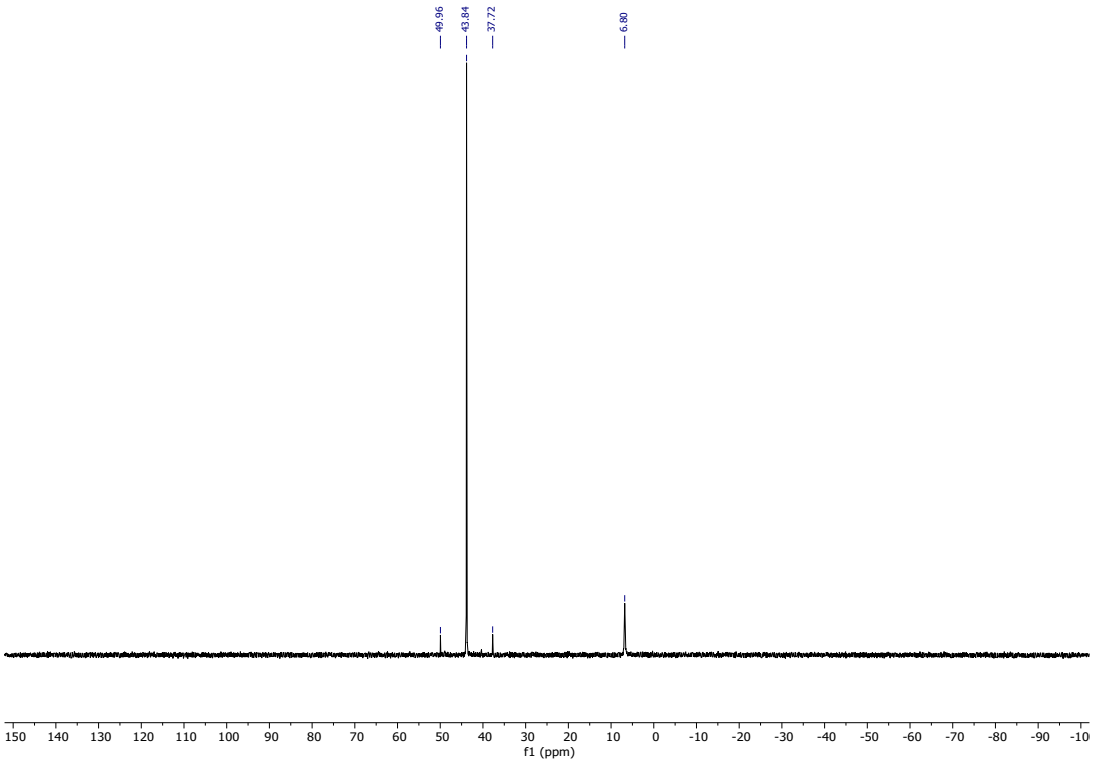


**Figure S6**. $^{31}P\{^{1}H\}$ NMR (121 MHz, $CD_2Cl_2$, 25 °C) spectrum of complex **2**.

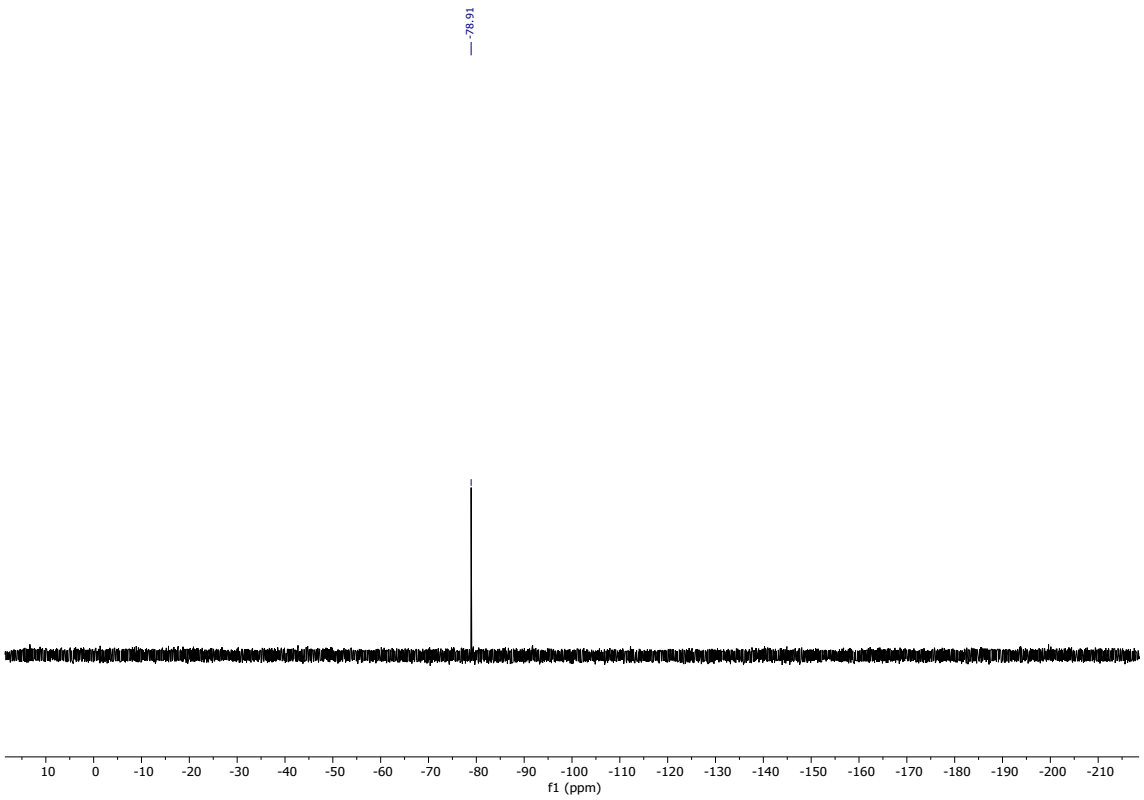


**Figure S7**. $^{19}F$ NMR (282 MHz, $CD_2Cl_2$, 25 °C) spectrum of complex **2**.

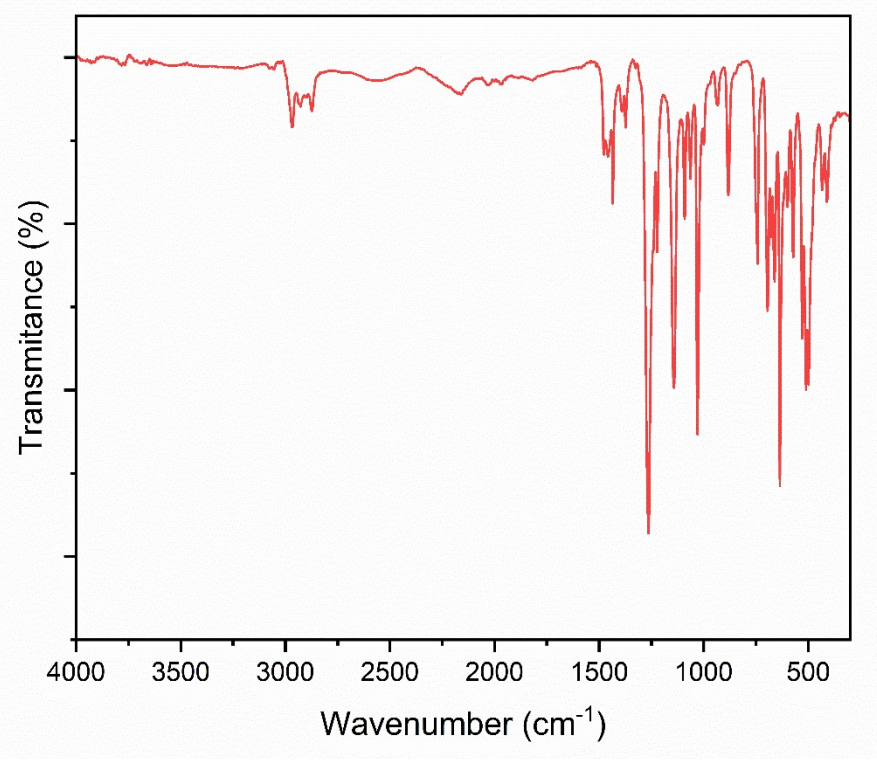


**Figure S8**. FTIR (ATR) spectrum of complex **2**.

**Complex 3**

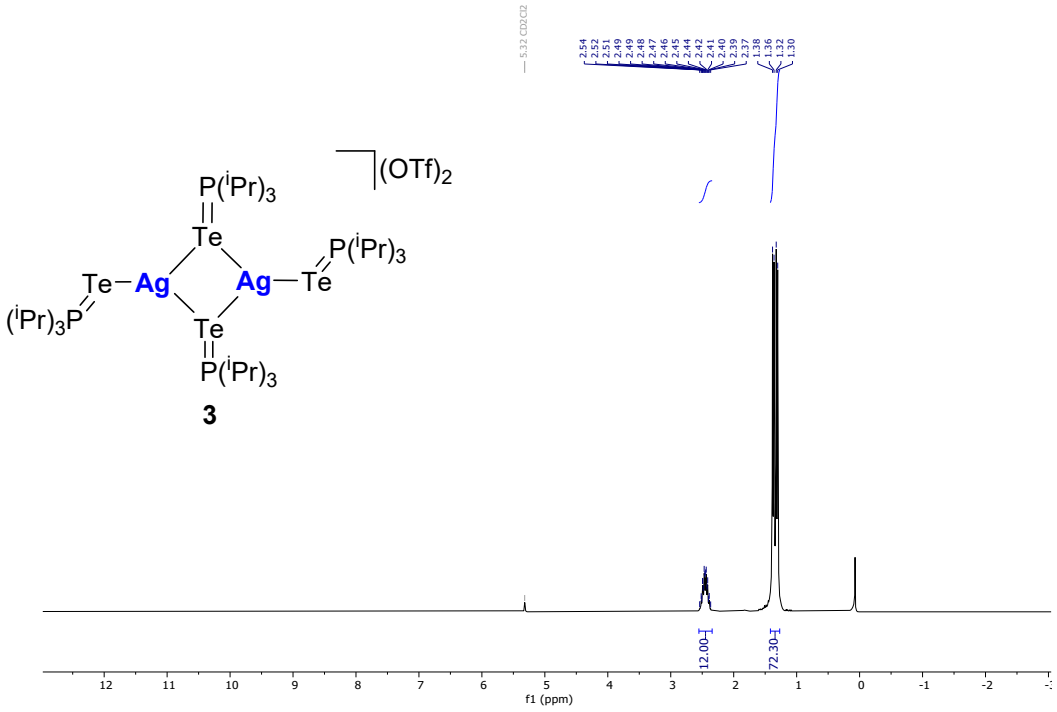


**Figure S9**. $^{1}H$ NMR (300 MHz, $CD_2Cl_2$, 25 °C) spectrum of complex **3**.

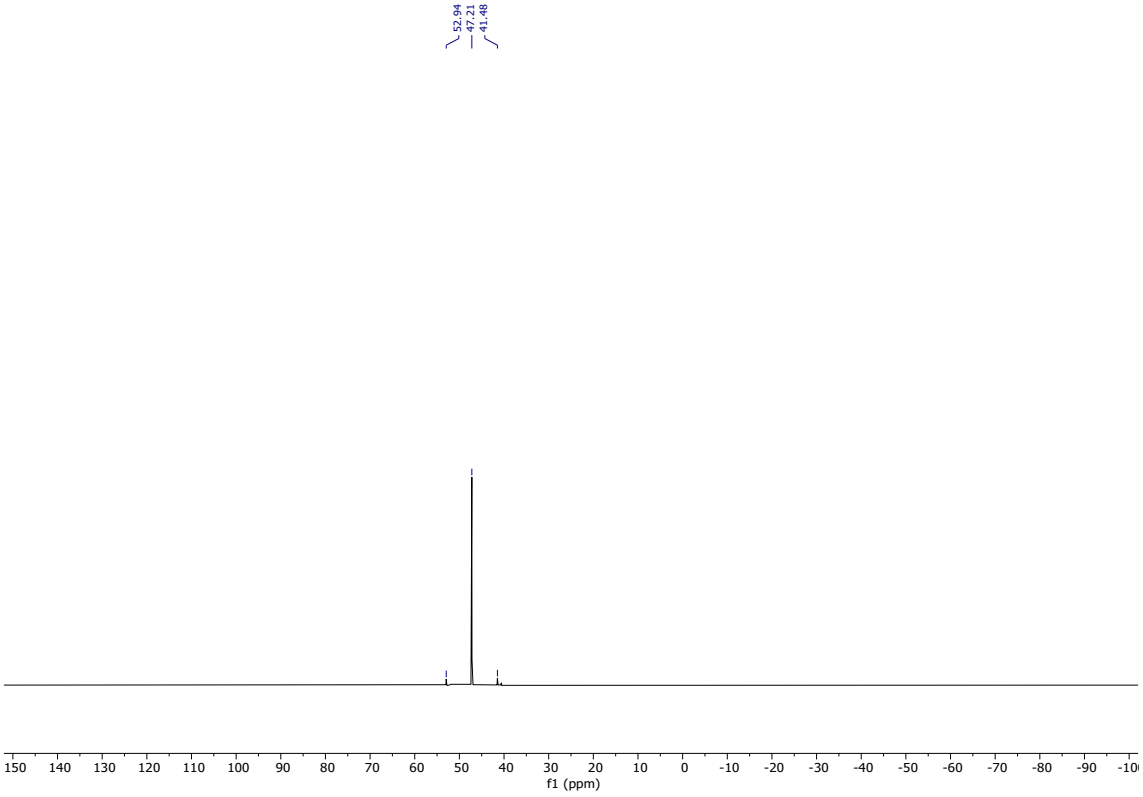


**Figure S10**. $^{31}P\{^{1}H\}$ NMR (121 MHz, $CD_2Cl_2$, 25 °C) spectrum of complex **3**.

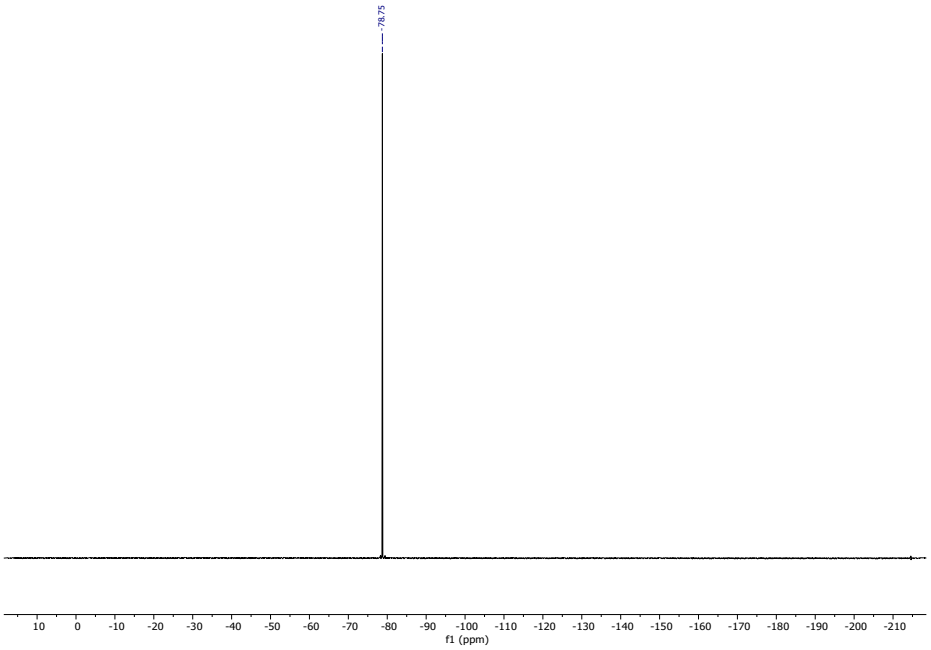


**Figure S11**. $^{19}F$ NMR (282 MHz, $CD_2Cl_2$, 25 °C) spectrum of complex **3**.

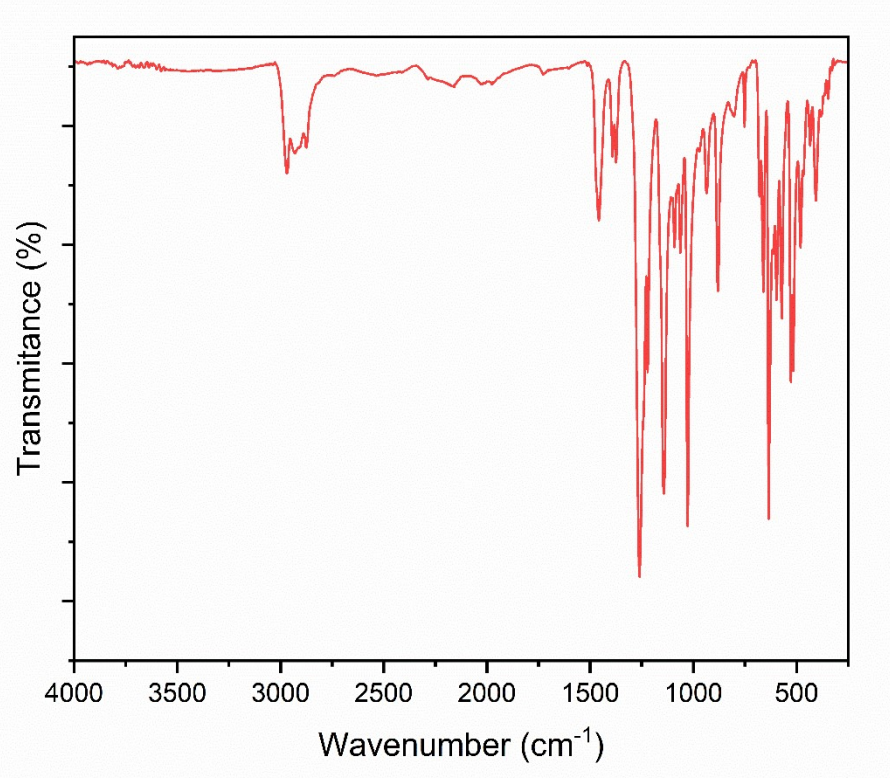


**Figure S12.** FTIR (ATR) spectrum of complex **3**.

DOSY experiments were carried out in $CD_2Cl_2$, at constant concentration of 5 mM.

The displayed diffusion coefficient is the result of calculating the average of the individual diffusion coefficients associated with each proton signal.

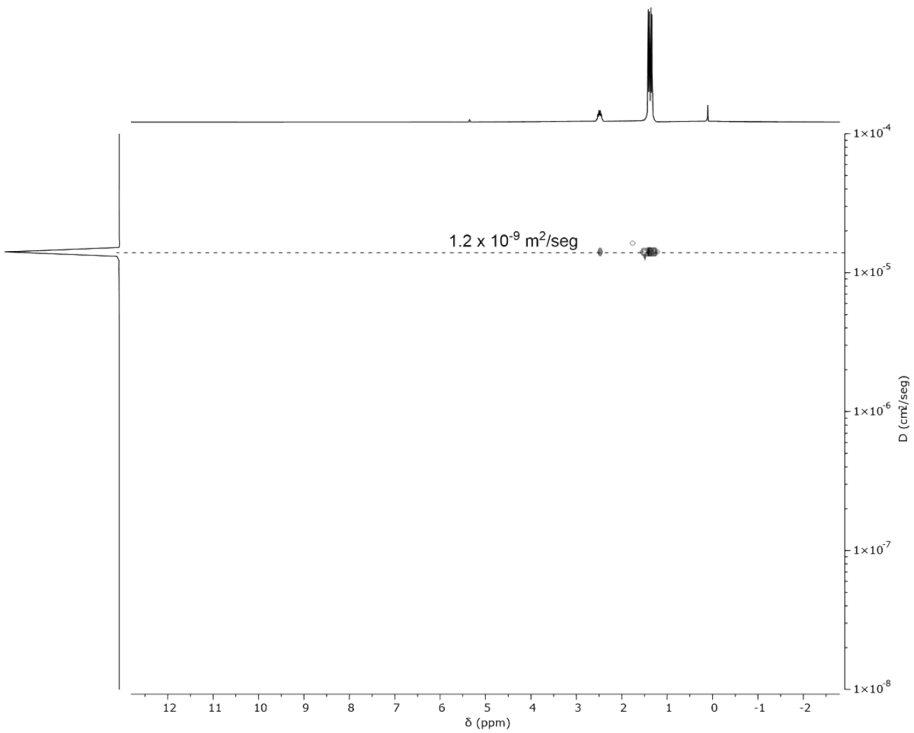


**Figure S13**. $^1$H DOSY NMR (500 MHz, $CD_2Cl_2$, 25 °C) spectrum of complex **3**.

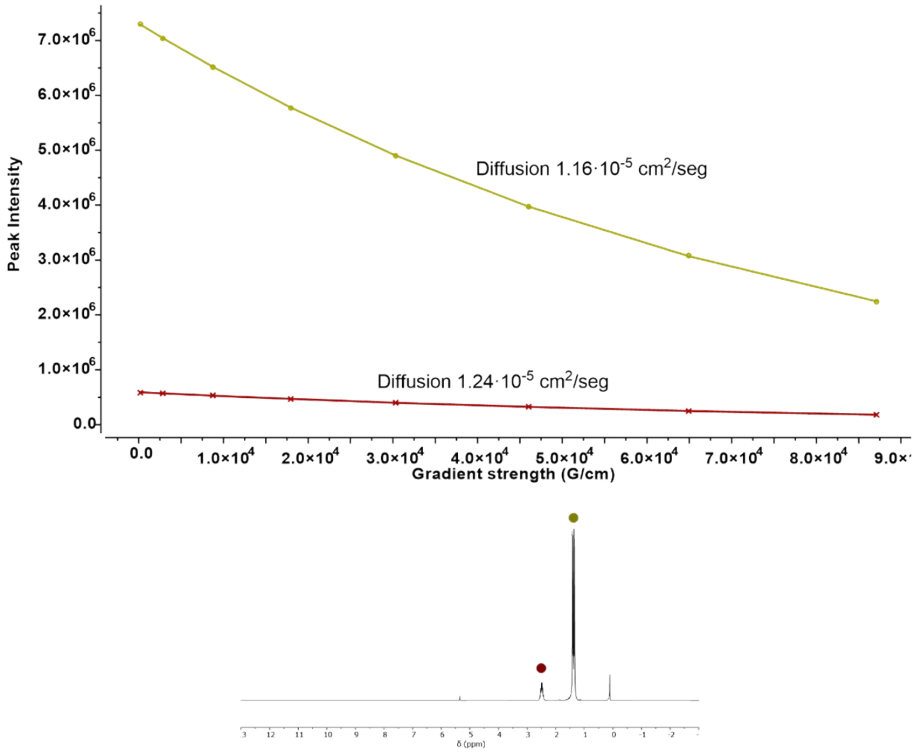


**Figure S14**. Diffusion coefficient calculations for $^1$H NMR signals of **3** as shown above.

**Complex 4**

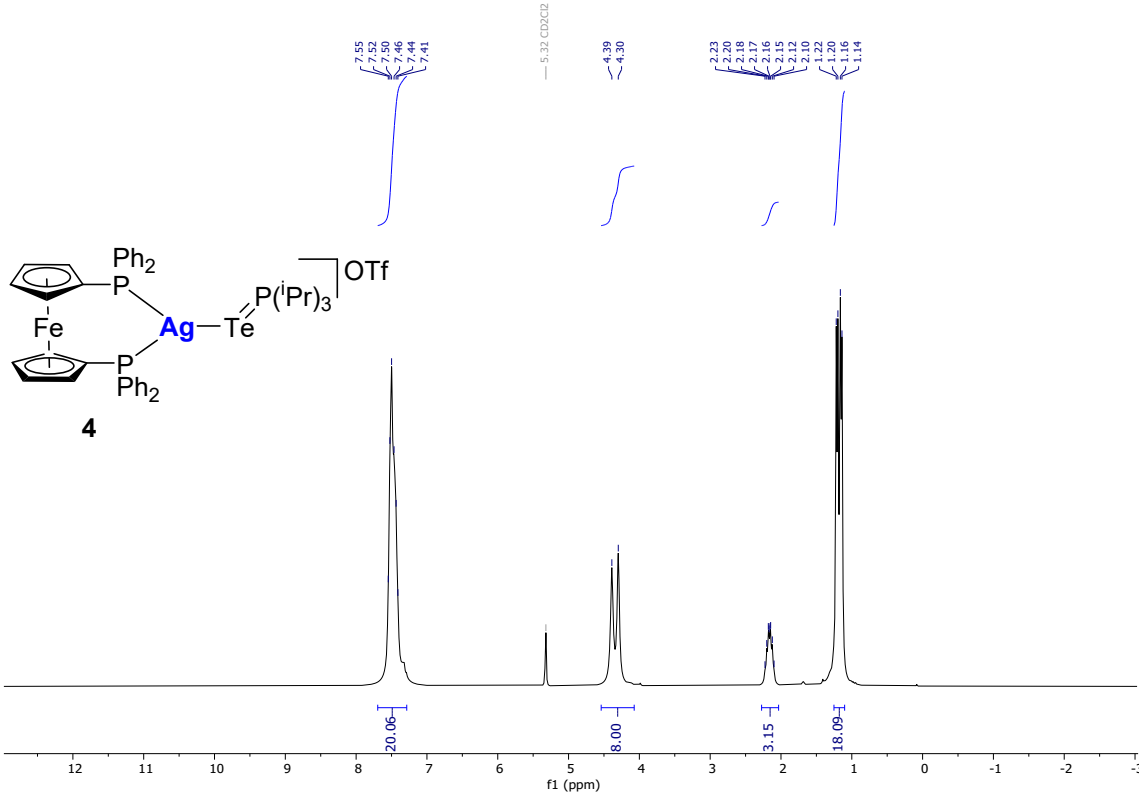


**Figure S15**. $^{1}H$ NMR (300 MHz, $CD_2Cl_2$, 25 °C) spectrum of complex **4**.

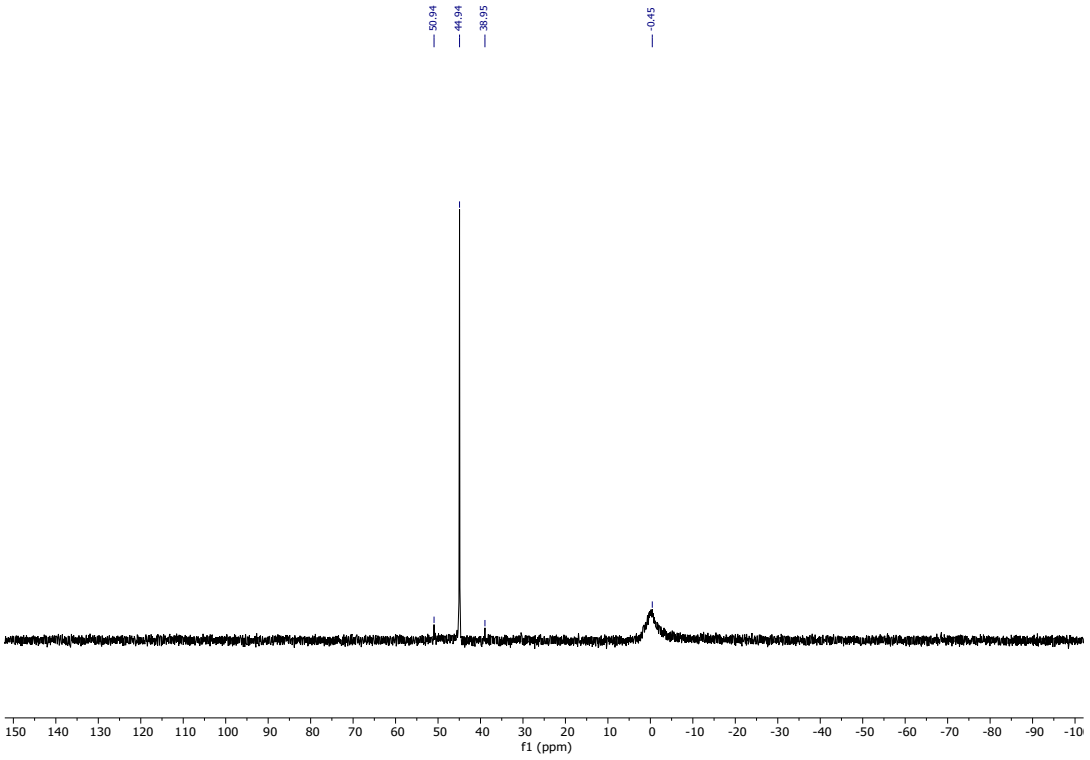


**Figure S16**. $^{31}P\{^{1}H\}$ NMR (121 MHz, $CD_2Cl_2$, 25 °C) spectrum of complex **4**.

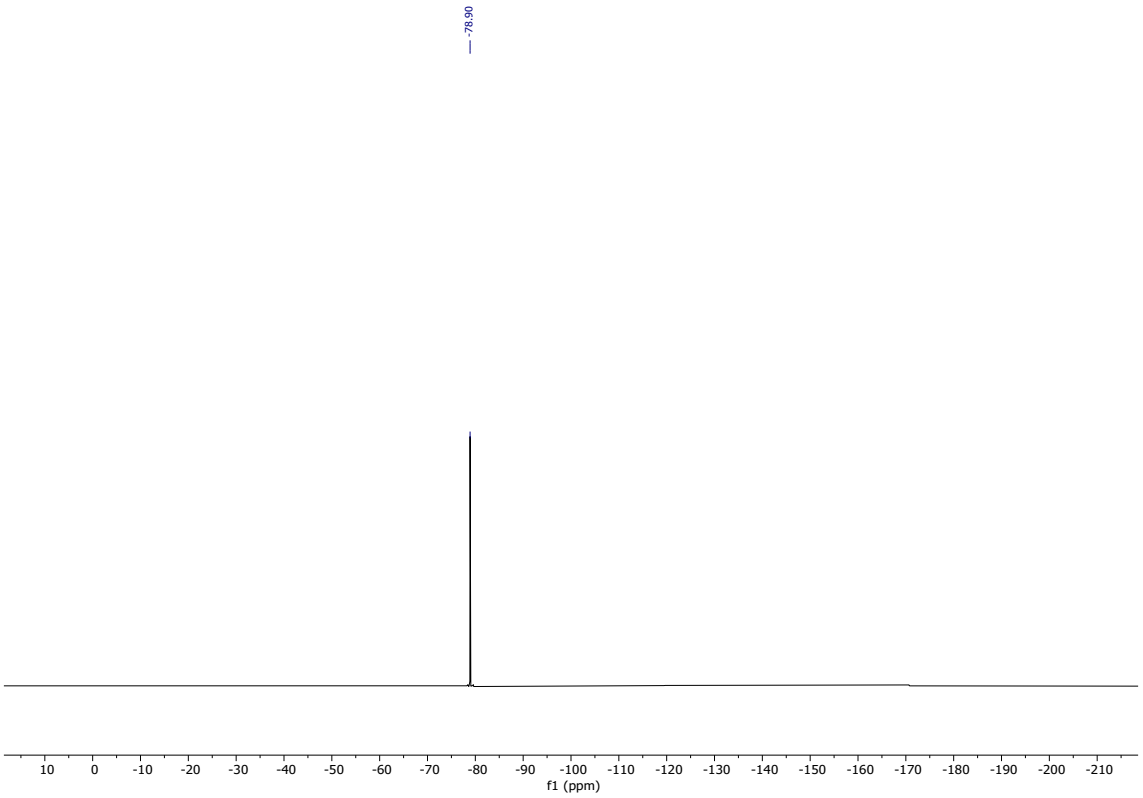


**Figure S17**. $^{19}F$ NMR (282 MHz, $CD_2Cl_2$, 25 °C) spectrum of complex **4**.

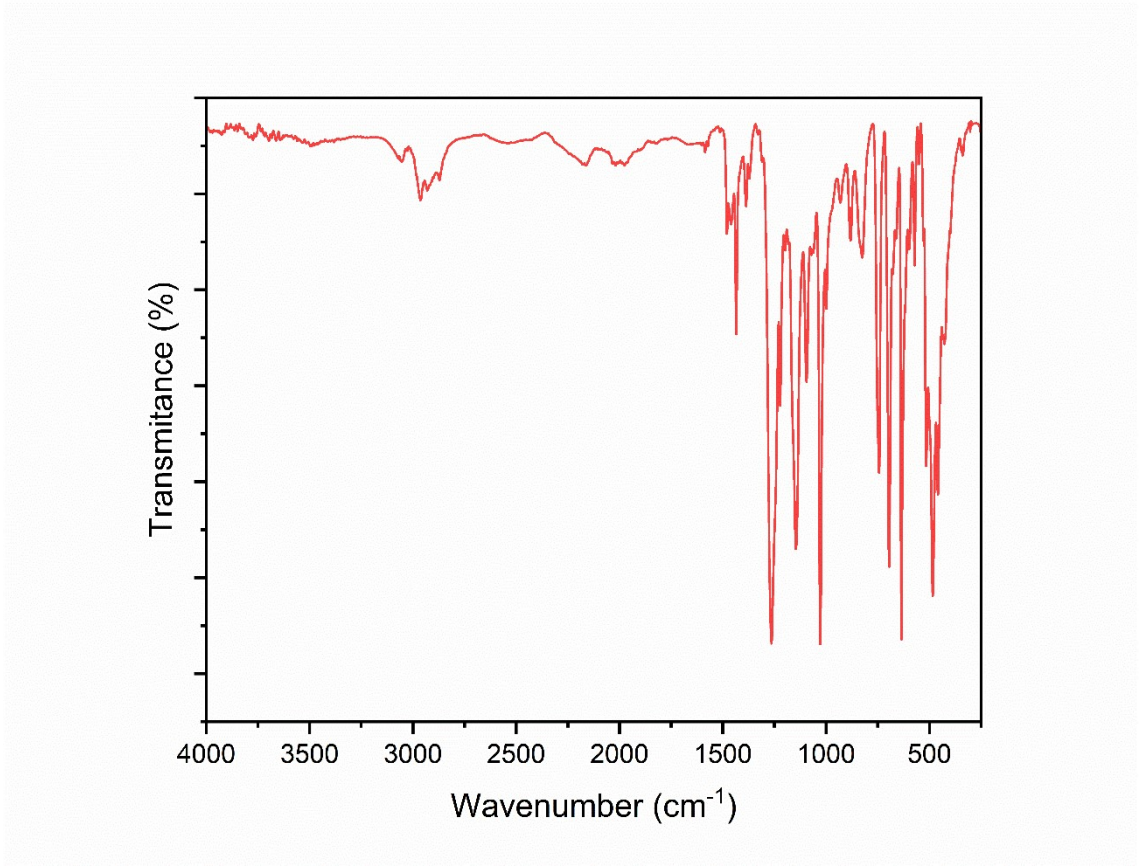


**Figure S18.** FTIR (ATR) spectrum of complex **4**.

**Complex 5**

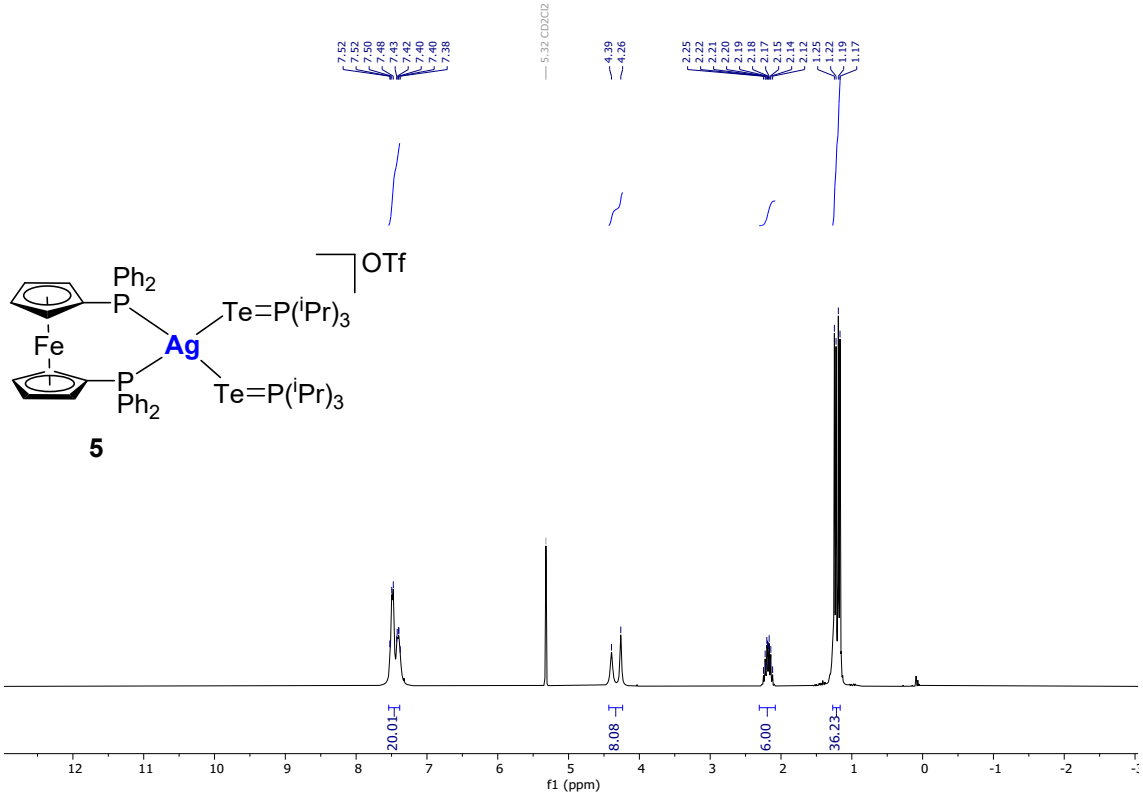


**Figure S19**. $^{1}H$ NMR (300 MHz, $CD_2Cl_2$, 25 °C) spectrum of complex **5**.

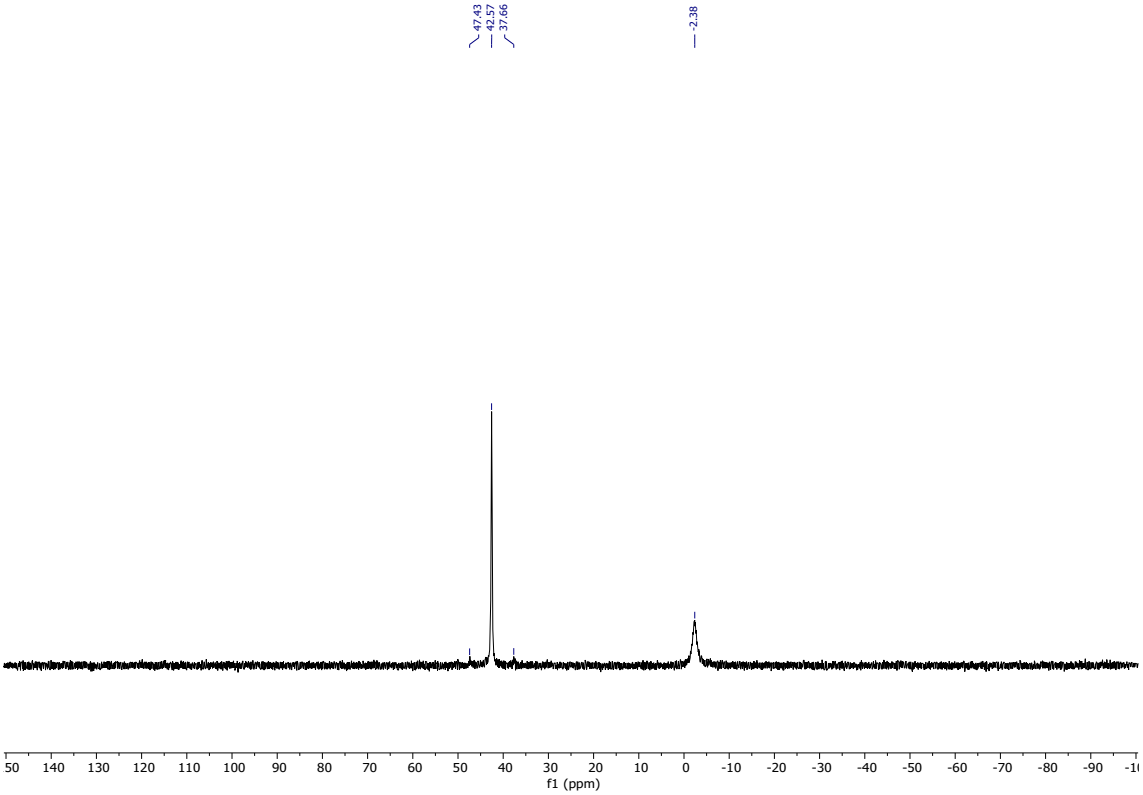


**Figure S20**. $^{31}P\{^{1}H\}$ NMR (121 MHz, $CD_2Cl_2$, 25 °C) spectrum of complex **5**.

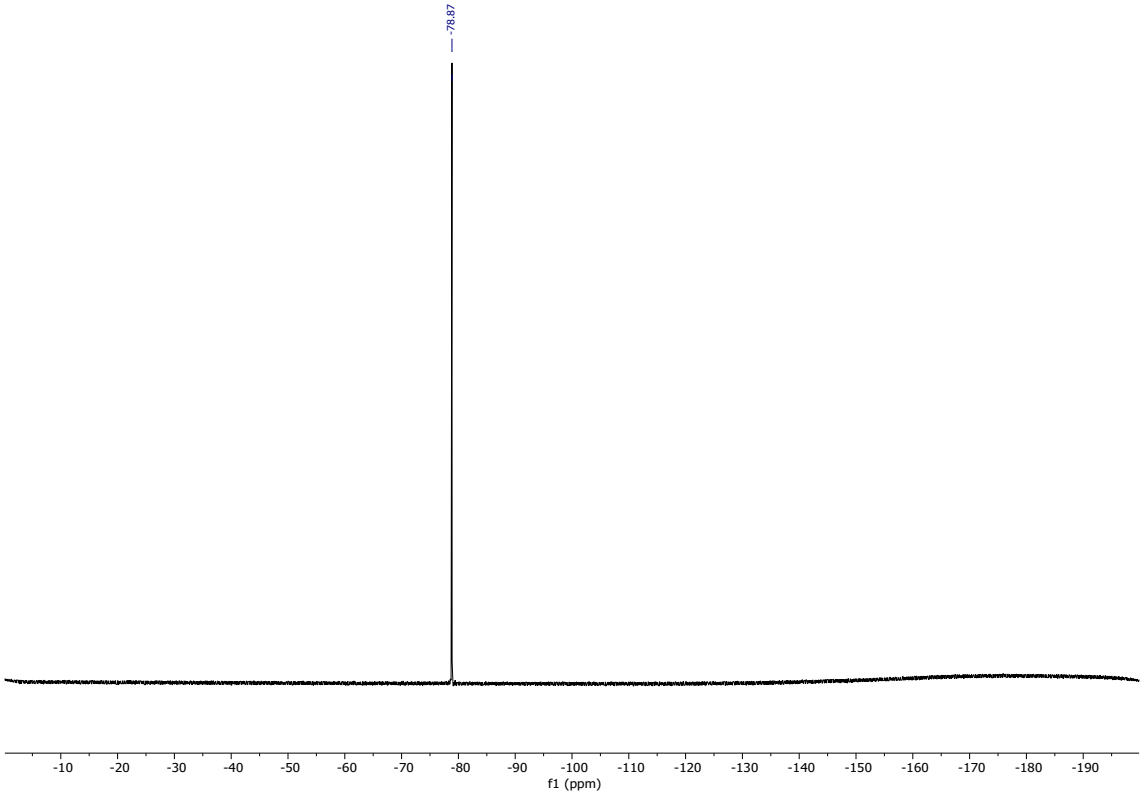


**Figure S21**. $^{19}F$ NMR (282 MHz, $CD_2Cl_2$, 25 °C) spectrum of complex **5**.

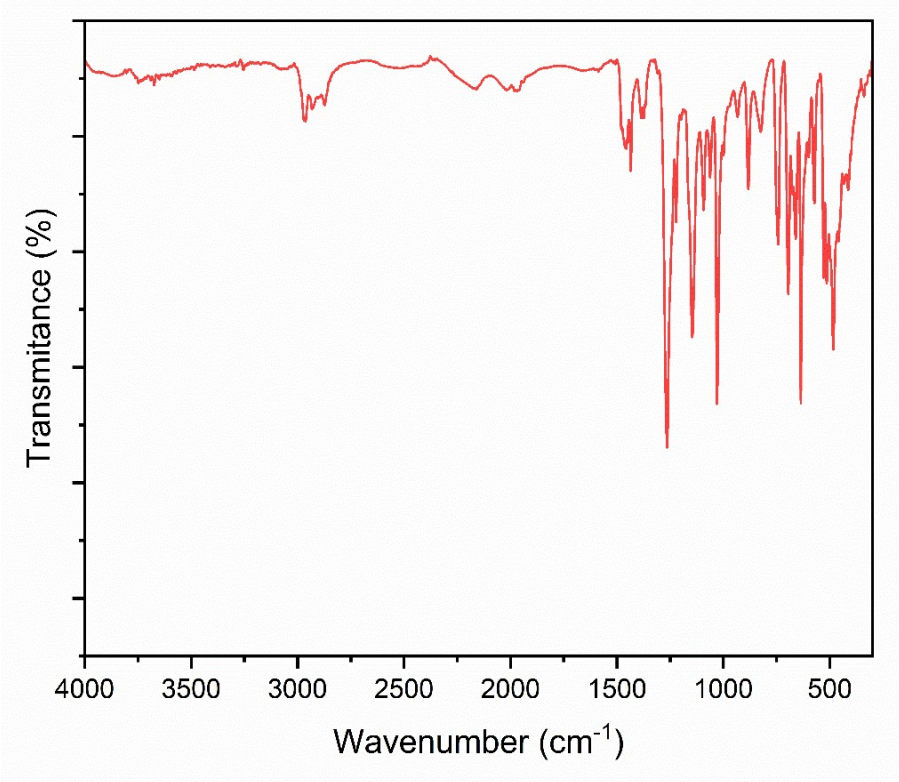


**Figure S22.** FTIR (ATR) spectrum of complex **5**.

# 3. HRMS Data

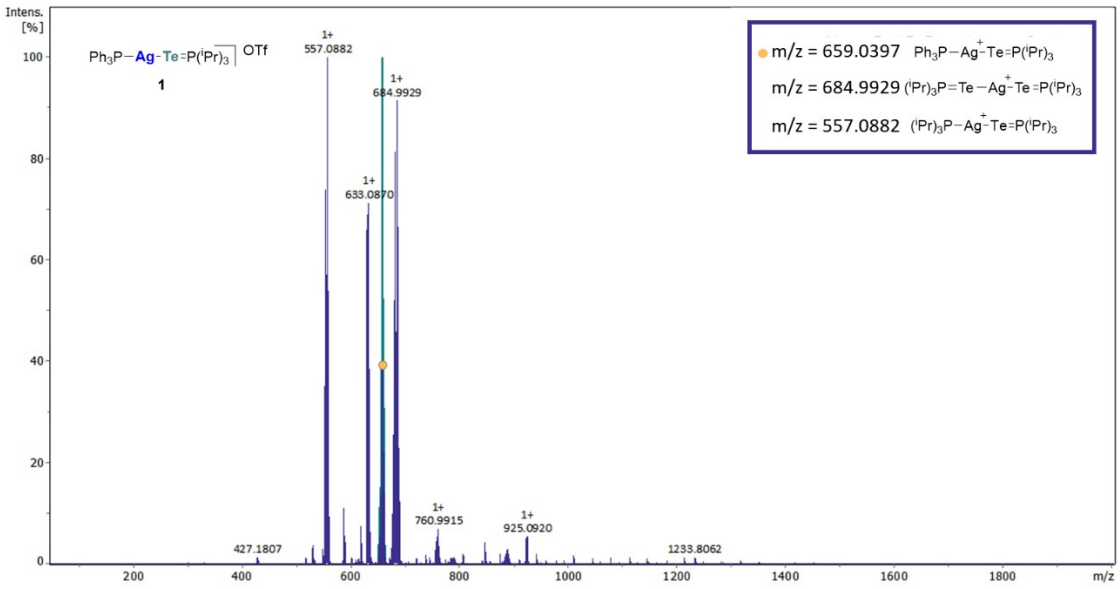


**Figure S23**. Mass Spectrum (ESI-QTOF) of complex **1**.

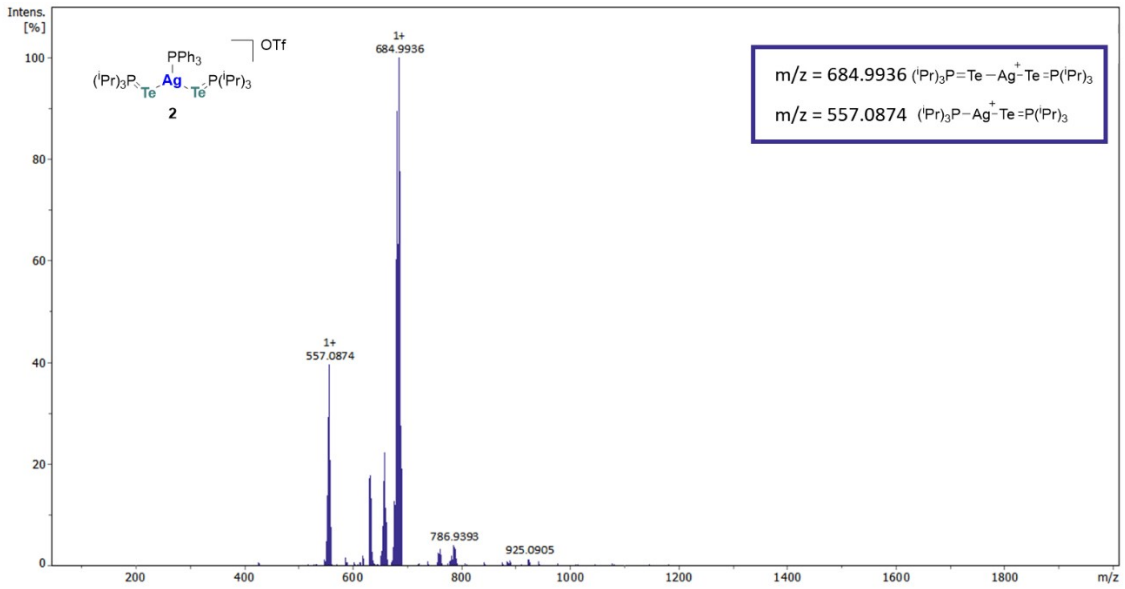


**Figure S24**. Mass Spectrum (ESI-QTOF) of complex **2**.

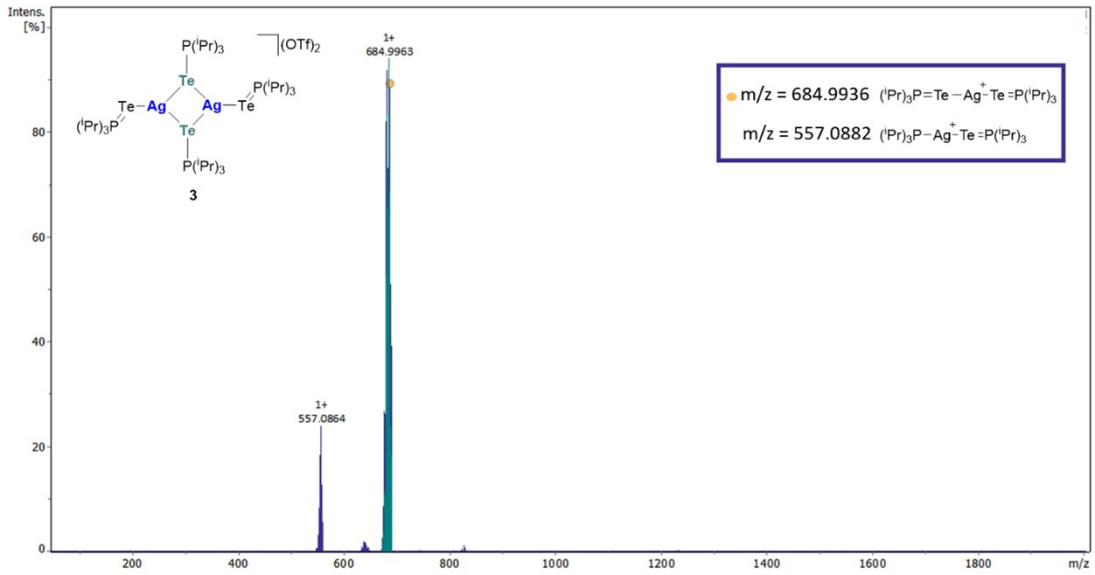


**Figure S25**. Mass Spectrum (ESI-QTOF) of complex **3**.

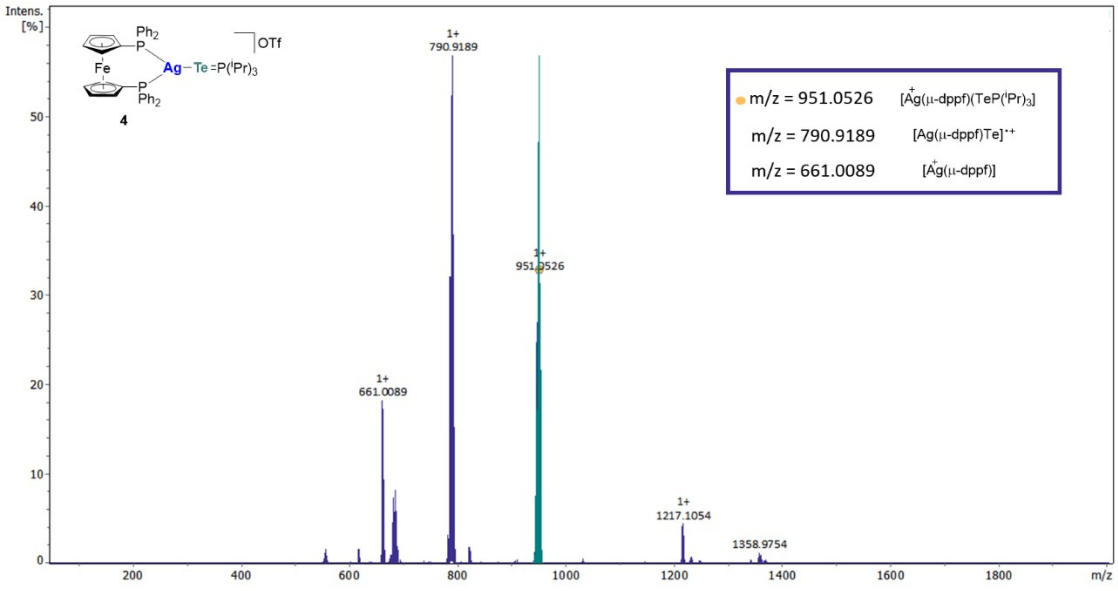


**Figure S26**. Mass Spectrum (ESI-QTOF) of complex **4**.

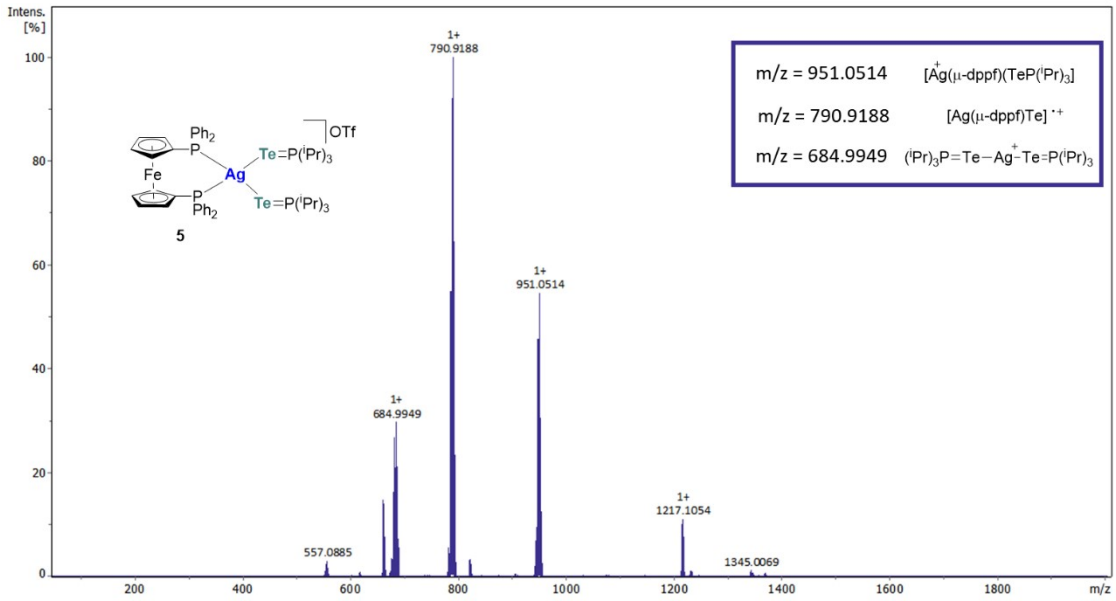


**Figure S27**. Mass Spectrum (ESI-QTOF) of complex **5**.

# 4. Electrochemical Studies

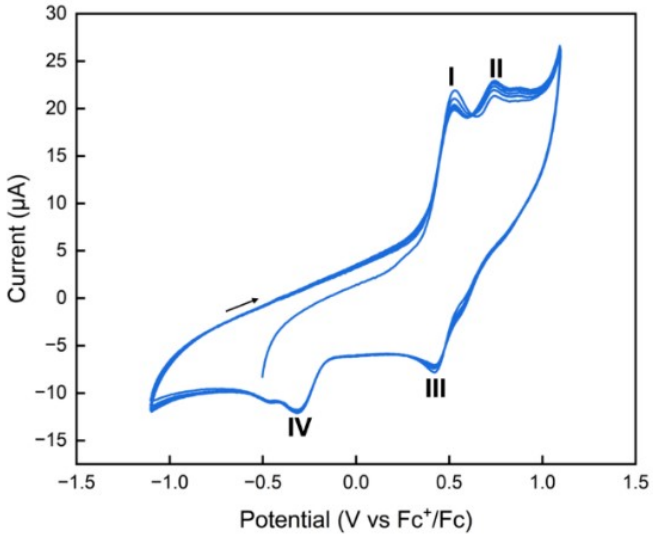


**Figure S28**. Cyclic voltammogram of complex **4** (0.5 mM) in dichloromethane (0.1 M $NBu_4PF_6$) acquired within a fixed potential window at a scan rate = 250 mV/s.

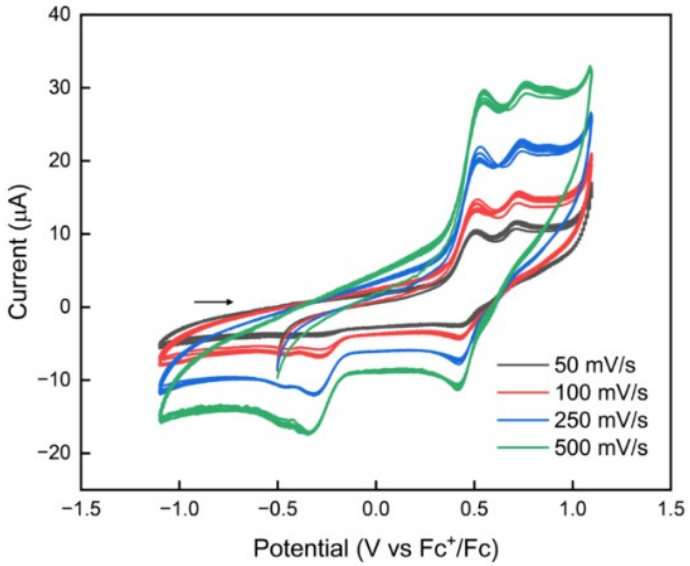


**Figure S29**. Cyclic voltammograms of complex **4** at varying scan rates (50 – 500 mV/s).

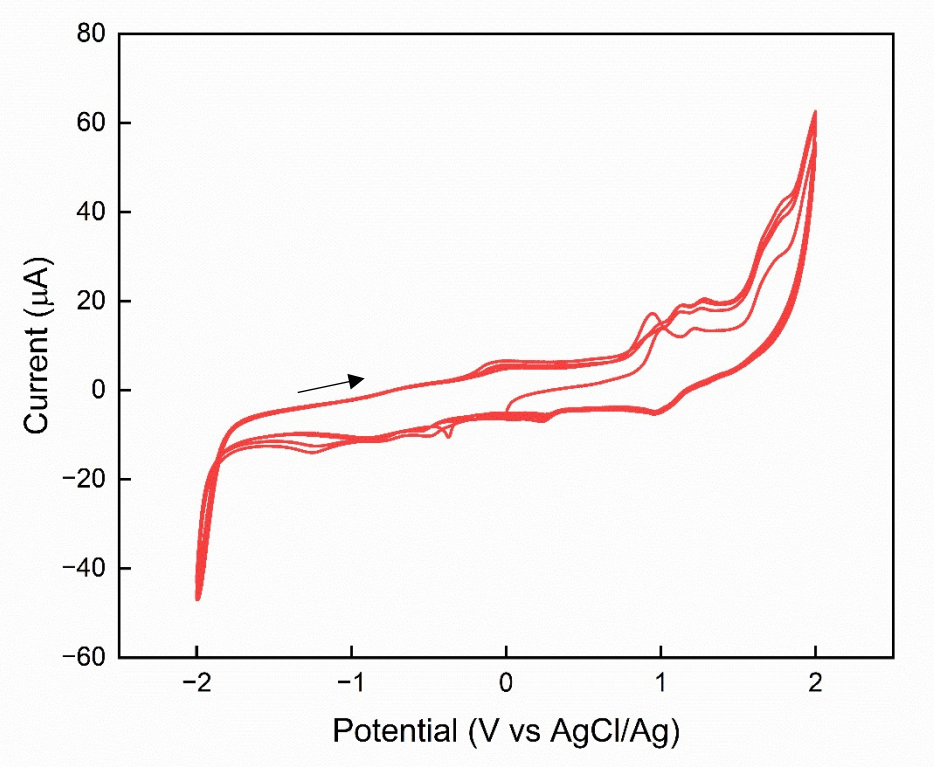


**Figure S30**. Cyclic voltammogram of a 0.5 mM solution of complex **4** in $CH_2Cl_2$/0.1M $[Bu_4N][PF_6]$ at 100 mV/s, in the electrochemical window of –2000 mV to 2000 mV, referenced against the AgCl/Ag electrode.

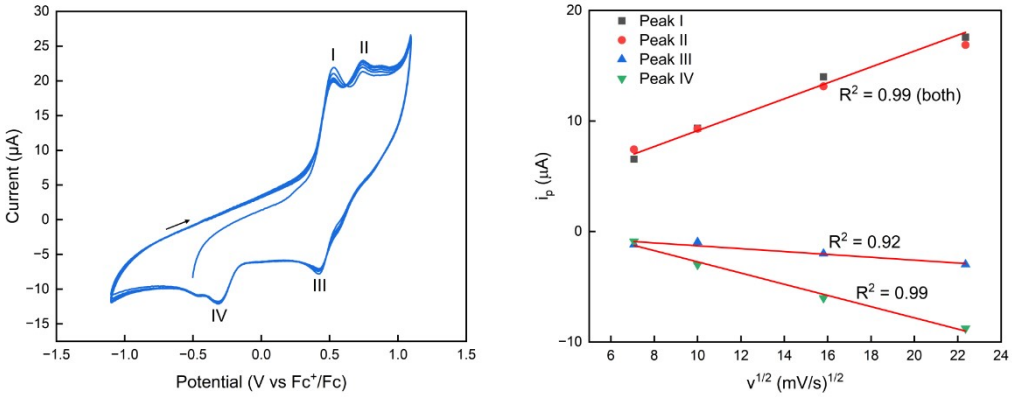


**Figure S31**. Relationship between peak current ($i_p$) and the square root of scan rate ($v^{1/2}$) (*Randles–Ševčík equation*) from cyclic voltammograms of a 0.5 mM solution of complex **4** in $CH_2Cl_2$/0.1M $[Bu_4N][PF_6]$ for all the peaks shown in the cyclic voltammogram. Linear fits are shown in red.

# 5. Crystal Data and Structure Refinement

**Table S1**. Crystal data and structure refinement for complex **3**

| | |
|---|---|
| Empirical Formula | $C_{76}\ H_{168}\ Ag_4\ F_{12}\ O_{12}\ P_8\ S_4\ Te_8$ |
| $M_t$ [g·mol$^{-1}$] | 3330.507 |
| Crystal system | Triclinic |
| Space group | $P\bar{1}$ |
| a [Å] | 14.343(1) |
| b [Å] | 17.1806(11) |
| c [Å] | 26.0797(17) |
| α [°] | 73.229(2) |
| β [°] | 86.136(2) |
| γ [°] | 71.106(2) |
| V [Å$^3$] | 5819.3 |
| Z, Z’ | Z = 2, Z’ = 1 |
| Density [g·cm$^{-3}$] | 1.901 |
| *T* [K] | 100(2) |
| μ [mm$^{-1}$] | 2.877 |
| *F*(000) | 3222.8 |
| 2θ range [°] | 4.38 to 56.62 |
| no. of collected reflections | 204541 |
| no. of unique reflections | 28854 |
| $R_{int}$ | 0.0419 |
| $R_1$, $wR_2$ [I > 2σ(I)][a] | $R_1$ = 0.0249, $wR_2$ = 0.0600 |
| $R_1$, $wR_2$ (all data)[a] | $R_1$ = 0.0267, $wR_2$ = 0.0609 |
| GOF ($F^2$)[b] | 1.052 |

[a] $R_1 = \Sigma(|F_o| - |F_c|) / \Sigma |F_o|$. $wR_2 = [\Sigma w (F_o^2 - F_c^2)^2 / \Sigma w(F_o^2)^2]^{1/2}$

[b] Goodness-of-fit = $[\Sigma w (F_o^2 - F_c^2)^2 / (n_{obs} - n_{param})]^{1/2}$

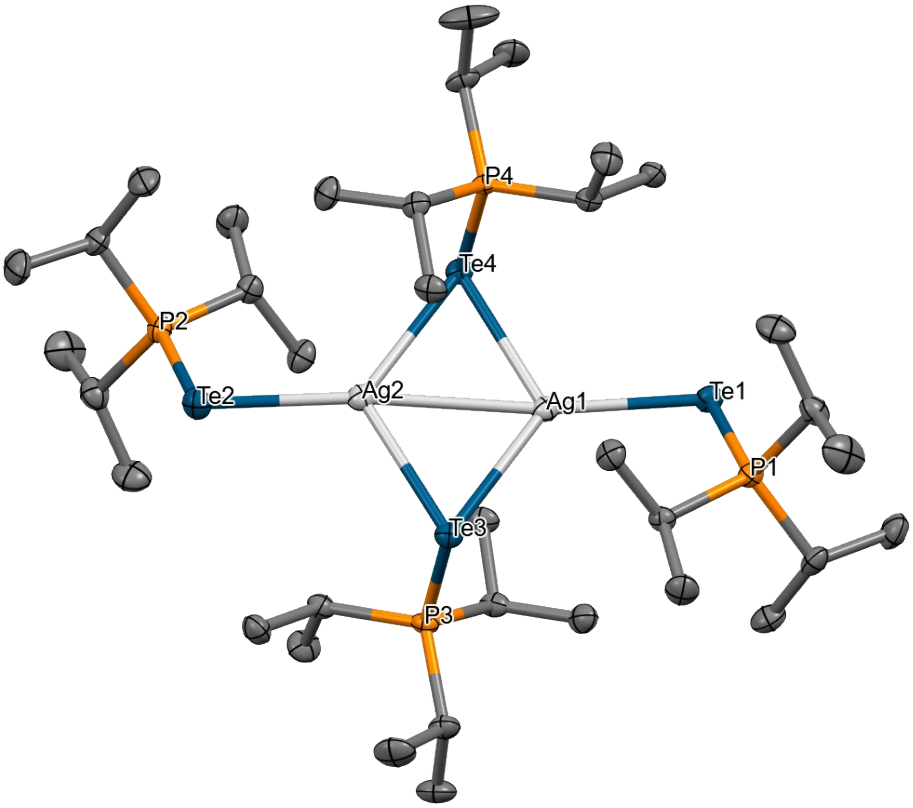


**Table S2**. Interatomic distances [Å] and angles [°] for complex **3** (one asymmetric molecule) with atom labelling as indicated above.

| | | | |
|---|---|---|---|
| Ag1–Ag2 | 3.0388(3) | Ag2–Te4–Ag1 | 65.47(1) |
| Ag1–Te1 | 2.7081(3) | Ag2–Te3–Ag1 | 65.35(1) |
| Ag1–Te3 | 2.8158(3) | P2–Te2–Ag2 | 101.33(2) |
| Ag1–Te4 | 2.7946(3) | P1–Te1–Ag1 | 101.16(2) |
| Ag2–Te2 | 2.7136(3) | Te4–Ag2–Te2 | 127.95(1) |
| Ag2–Te3 | 2.8128(3) | Te4–Ag1–Te1 | 115.65(1) |
| Ag2–Te4 | 2.8244(3) | Te3–Ag2–Te2 | 117.79(1) |
| P1–Te1 | 2.4038(7) | Te3–Ag1–Te1 | 129.25(1) |
| P2–Te2 | 2.4063(8) | Te2–Ag2–Ag1 | 174.27(1) |
| P3–Te3 | 2.4164(6) | Te1–Ag1–Ag2 | 172.92(1) |
| P4–Te4 | 2.4157(6) | Te4–Ag1–Te3 | 115.01(1) |
| | | Te4–Ag2–Te3 | 114.16(1) |

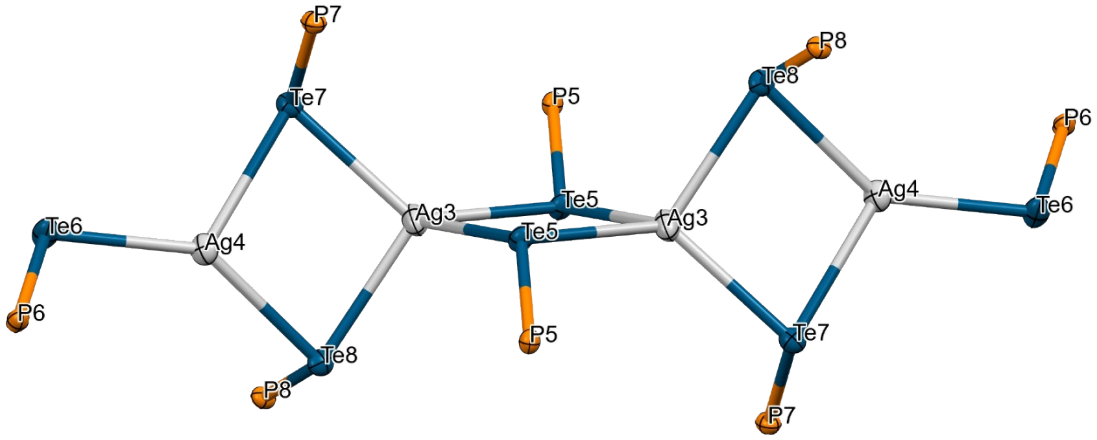


**Table S3**. Interatomic distances [Å] and angles [°] for complex **3** (one asymmetric molecule) with atom labelling as indicated above.

| | | | |
|---|---|---|---|
| P6–Te6 | 2.4149(6) | Ag3–Ag3 | 4.2850(4) |
| Te6–Ag4 | 2.6877(4) | Ag3–Te7 | 2.8067(4) |
| Ag4–Te7 | 2.8791(3) | Ag3–Te8 | 2.8267(3) |
| Ag4–Te8 | 2.7757(3) | Ag3–Ag4 | 3.6178(4) |
| Ag3–Te8 | 2.8267(3) | Ag4–Te7 | 2.8791(3) |
| Ag3–Te7 | 2.8067(4) | Ag4–Te8 | 2.7757(3) |
| Ag4–Ag3 | 3.6178(4) | Ag4–Te6 | 2.6877(4) |
| P8–Te8 | 2.4133(6) | Ag4–Te8–Ag3 | 80.44(1) |
| P7–Te7 | 2.4090(6) | Te8–Ag4–Te7 | 98.38(1) |
| Ag3–Te5 | 2.7615(3) | Ag3–Te5–Ag3 | 96.78(1) |
| P5–Te5 | 2.4246(6) | Te5–Ag3–Te5 | 83.22(1) |
| | | Ag3–Te7–Ag4 | 79.02(1) |
| | | Te7–Ag3–Te8 | 98.91(1) |

**Table S4**. Crystal data and structure refinement for complex **4**

| | |
|---|---|
| Empirical Formula | $C_{44}\ H_{49}\ Ag\ F_3\ Fe\ O_3\ P_3\ S\ Te$ |
| $M_t$ [g·mol$^{-1}$] | 1099.177 |
| Crystal system | Monoclinic |
| Space group | $P2_1/n$ |
| a [Å] | 17.4423(6) |
| b [Å] | 13.6680(5) |
| c [Å] | 19.5183(7) |
| α [°] | 90 |
| β [°] | 109.7270(10) |
| γ [°] | 90 |
| V [Å$^3$] | 4380.1 |
| Z, Z' | Z = 4, Z' = 1 |
| Density [g·cm$^{-3}$] | 1.662 |
| $T$ [K] | 100(2) |
| μ [mm$^{-1}$] | 1.640 |
| $F$(000) | 2200.2 |
| 2θ range [°] | 3.844 to 50.998 |
| no. of collected reflections | 116808 |
| no. of unique reflections | 8144 |
| $R_{int}$ | 0.0368 |
| $R_1$, $wR_2$ [I > 2σ(I)][a] | $R_1$ = 0.0236, $wR_2$ = 0.0569 |
| $R_1$, $wR_2$ (all data)[a] | $R_1$ = 0.0244, $wR_2$ = 0.0574 |
| GOF ($F^2$)[b] | 1.038 |

[a] $R_1 = \Sigma(|F_o| - |F_c|) / \Sigma |F_o|$. $wR_2 = [\Sigma w (F_o^2 - F_c^2)^2 / \Sigma w(F_o^2)^2]^{1/2}$

[b] Goodness-of-fit = $[\Sigma w (F_o^2 - F_c^2)^2 / (n_{obs} - n_{param})]^{1/2}$

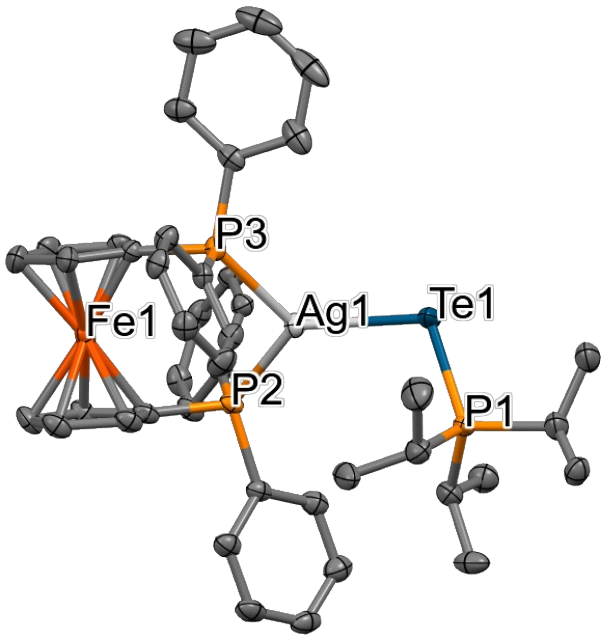


**Table S5**. Interatomic distances [Å] and angles [°] for complex **4** with atom labelling as indicated above.

| | |
|---|---|
| Ag1–Te1 | 2.71059(5) |
| Ag1–P2 | 2.4681(7) |
| Ag1–P3 | 2.5061(7) |
| Te1–P1 | 2.4034(6) |
| P3–Ag1–P2 | 110.53(2) |
| P3–Ag1–Te1 | 120.45(2) |
| Ag1–Te1–P1 | 106.92(2) |
| P2–Ag1–Te1 | 128.96(2) |

# 6. References


1 M. Bardají, O. Crespo, A. Laguna and A. K. Fischer, *Inorg. Chim. Acta,* 2000, **304**, 7–16.

2 X. L. Lu, W. K. Leong, T. S. A. Hor and L. Y. Goh, *J. Organomet. Chem.*, 2004, **689**, 1746–1756.

3 N. Kuhn, G. Henkel, H. Schumann and R. Froehlich, *Z. Naturforsch. Teil B,* 1990, **45**, 1010–1018.

4 G. M. Sheldrick, *SADABS, Program for adsorption correction*, University of Göttingen, Göttingen, Germany, 1996.

5 a) O. V. Dolomanov, L. J. Bourhis, R. J. Gildea, J. A. K. Howard and H. Puschmann, *J. Appl. Crystallogr*., 2009, **42**, 339–341; b) L. J. Bourhis, O. V. Dolomanov, R. J. Gildea, J. A. K. Howard and H. Puschmann, *Acta Cryst. A*, 2015, **A71**, 59-71.